Direct search of dark matter in high-scale supersymmetry

Junji Hisano, Koji Ishiwata, and Natsumi Nagata

Phys. Rev. D **87**, 035020 — Published 15 February 2013

DOI: 10.1103/PhysRevD.87.035020

IPMU 12-0187
CALT 68-2891

Direct Search of Dark Matter in High-Scale Supersymmetry

Junji Hisano[a,b], Koji Ishiwata[c] and Natsumi Nagata[a,d]

[a] *Department of Physics, Nagoya University, Nagoya 464-8602, Japan*
[b] *Kavli IPMU, University of Tokyo, Kashiwa 277-8584, Japan*
[c] *California Institute of Technology, Pasadena, CA 91125, USA*
[d] *Department of Physics, University of Tokyo, Tokyo 113-0033, Japan*

Abstract

We study direct detection of dark matter in supersymmetric (SUSY) model where most of SUSY particles have very high-scale masses beyond the weak scale. In the scenario, Wino-like or Higgsino-like neutralino is a good candidate for the dark matter in the universe. The neutralino scatters off nuclei by a Higgs-boson exchange diagram and also electroweak loop diagrams. It is found that the elastic-scattering cross section with nuclei is enhanced or suppressed due to constructive or deconstructive interference among the diagrams. Such a cross section is within the reach of future experiment in some parameter region.

1 Introduction

Supersymmetric (SUSY) remodelling of the Standard Model (SM) is one of the promising candidates for physics beyond the SM. The minimal extension, called the minimal supersymmetric Standard Model (MSSM), has been studied enthusiastically in various literature. The weak-scale SUSY is, however, severely constrained by the experiments at the Large Hadron Collider (LHC). Since no signal of SUSY particles has been discovered yet, the ATLAS and the CMS Collaborations have imposed stringent limits on their masses, especially those of colored particles [1]. The weak-scale SUSY is also challenged by the discovery of the SM-like Higgs boson with a mass of about 125 GeV, which is recently reported by the collaborations [2]. In the MSSM radiative corrections from heavy sfermions make the Higgs mass larger [3]. Thus those results from the LHC may indicate that the SUSY scale is somewhat higher than the weak scale [4].

Although the high-scale SUSY scenario sounds unnatural in a viewpoint of the hierarchy problem, phenomenological aspects of heavy sfermions are quite fascinating [5–11]. Due to the sufficient radiative corrections, the 125 GeV Higgs boson may be achieved [12]. The SUSY contributions to flavor changing neutral current (FCNC) processes and electric dipole moments are suppressed by heavy sfermion masses so that the SUSY flavor and CP problems are relaxed [13]. In cosmology, the gravitino problem may be avoided because it may be as heavy as sfermions, then the thermal leptogenesis for baryon asymmetry in the universe works with high reheating temperature [14]. On top of that, the gauge coupling unification is achieved as precisely as that in the MSSM since the sfermions form the SU(5) multiplets, and the proton lifetime could be well above the current experimental limit [15]. These features have stimulated various works [16].

The high-scale SUSY scenario does not necessarily mean all SUSY particles in the MSSM are heavy. Superpartners of gauge bosons and Higgs bosons may be at the weak scale without destroying above features. This is plausible because the lightest particle among their mixed states is the lightest SUSY particle (LSP) and it is a good candidate for the dark matter (DM) in the universe. Such a candidate is one of so-called Weakly Interacting Massive particles (WIMPs). Though sfermions may be beyond the reach of the LHC, the LSP DM may be searched in the direct dark-matter detection experiments.

In this article we consider a scenario where the LSP mass is around the weak scale and the other SUSY particles are much heavier, and give a precise calculation of elastic-scattering cross section between the LSP DM and nucleon. Wino-like or Higgsino-like neutralino is a viable DM candidate since the thermal production in the early hot universe gives the observed DM density even in the heavy sfermion scenario; Wino with a mass of 2.7–3.0 TeV [17] or Higgsino with a mass of 1 TeV [18]. The neutralino mass less than TeV is also possible to explain the the DM density when its non-thermal production is considered [19, 20]. Also the Wino LSP is a natural consequence of the anomaly mediation [21]. Therefore we focus on those well-motivated cases. Since there are only a few undetermined parameters, the observed value of the Higgs-boson mass at 125 GeV allows us to make a robust prediction for the scattering cross section with nucleon. As we will see below, both the tree-level [22, 23] and the loop-level processes [24–26] give rise

to sizable contributions to the scattering cross section.

This paper is organized as follows. In the next section, we explain the scenario of high-scale supersymmetry, in which the Wino-like or Higgsino-like neutralino is predicted as the DM. In Section 3, the effective Lagrangian for the neutralino-nucleon elastic scattering is reviewed. In Section 4, we discuss relevant tree and loop-level contributions to the spin-independent (SI) scattering of the Wino-like or Higgsino-like neutralino, and evaluate the cross section. Section 5 is devoted to conclusion. In the evaluation of the SI cross section in text, we use the results of the lattice QCD simulations for the mass fractions of light quarks in nucleon. We also show the results when the mass fractions estimated in the chiral perturbation theory are used in Appendix A. In Appendix B, we give the spin-dependent (SD) cross section for completeness.

2 The Scenario

In this section we briefly describe the scenario which we discuss in this paper. As it is mentioned in the Introduction, we consider a SUSY scenario where all SUSY particles are well above the weak scale, except for Wino or Higgsino. Such mass spectrum is given by a simple SUSY breaking mechanism [5, 6, 11, 21]. Assume that there exists a SUSY breaking hidden sector containing a SUSY breaking field Z which is charged under some symmetry. Then a generic form of Kähaler potential yields masses of $M_{\rm SUSY} \sim F_Z/M_*$ for all the scalar bosons in the MSSM except the lightest Higgs boson (F_Z and M_* are the F-component vacuum expectation value (VEV) of the field Z and the messenger scale, respectively). On the other hand, since Z is charged under some symmetry, the gaugino and Higgsino mass terms are not given by the Z-field linear terms. Thus they do not necessarily have the mass scale $M_{\rm SUSY}$, *i.e.*, they are model-dependent.[1] Now we consider the case of $M_* = M_{\rm Pl}$ ($M_{\rm Pl}$ is the reduced Planck scale). In the case, gauginos acquire their masses via the anomaly mediation, which are of the order of $m_{3/2}/16\pi^2$. Here $m_{3/2} = F_Z/\sqrt{3}M_{\rm Pl}$ is the gravitino mass. For Higgsino, on the other hand, so-called μ term, $\mu H_u H_d$ in the superpotential (H_u and H_d are up-type and down-type Higgs chiral superfields, respectively), may be absent by a certain symmetry, *e.g.*, the Peccei-Quinn symmetry [27]. In such a case, the gaugino-Higgs loops induce the Higgsino mass, which is smaller than the gaugino masses by another loop factor. Thus, the Higgsino-like neutralino is the LSP. On the contrary it may be as heavy as gravitino in another case. When the Kähaler potential has a term, $K = \kappa H_u H_d + \cdots$, the Higgsino mass is provided by the supergravity effects and it lies around the gravitino mass scale. In that case, the Wino-like neutralino is the LSP.

In order to consider the Wino-like or Higgsino-like neutralino, we take the Wino and Higgsino mass parameters as free parameters. Namely, the gaugino and Higgsino mass

[1] Trilinear soft SUSY breaking terms are also model-dependent. However, they are irrelevant in our discussion.

terms are given by

$$\mathcal{L}_{\rm ino}^{M} = -\sum_{a=1,2,3}\frac{1}{2}M_a\tilde{\lambda}_a\tilde{\lambda}_a - \mu\tilde{H}_u\tilde{H}_d, \tag{1}$$

where $\tilde{H}_u\tilde{H}_d = \tilde{H}_u^+\tilde{H}_d^- - \tilde{H}_u^0\tilde{H}_d^0$ and

$$M_a = \frac{b_a g_a^2}{16\pi^2}m_{3/2}. \tag{2}$$

Here $\tilde{\lambda}_a (a = 1, 2 \text{ and } 3)$ are Bino, Wino and Gluino, respectively, and $\tilde{H}_u$ and $\tilde{H}_d$ are up-type and down-type Higgsinos, respectively. The coefficients b_a denote the one-loop beta-functions of the gauge coupling constants g_a ($a = 1, 2$ and 3 for $\mathrm{U}(1)_Y$, $\mathrm{SU}(2)_L$ and $\mathrm{SU}(3)_C$, respectively) given by $(b_1, b_2, b_3) = (33/5, 1, -3)$.[2] After the electroweak symmetry breaking, Bino ($\tilde{B}$), Wino ($\tilde{W}^0$), and neutral Higgsinos mix with each other. The mass eigenstates, called neutralinos, are obtained as $\tilde{\chi}_i^0 = \sum_j Z_{ij}\chi_j^0$, where $\chi_i^0 = \tilde{B}, \tilde{W}^0, \tilde{H}_u^0$ and $\tilde{H}_d^0$ for $i = 1, 2, 3$ and 4, respectively. $\tilde{\chi}_1^0$ is the lightest neutralino, and from now on, we omit the subscript of $\tilde{\chi}_1^0$ for simplicity. In the following calculation we take M_2 as a free parameter instead of $m_{3/2}$, and consider the case where the lightest neutralino explains the current relic density of DM.

When sfermions are very heavy, the 125 GeV SM-like Higgs boson is achieved with $\tan\beta \sim 1$–5 [12]. Here $\tan\beta$ is the ratio of the VEVs of up- and down-type Higgs fields. In this article, however, we also consider larger $\tan\beta$ to demonstrate the cross section for general case, assuming appropriate sfermion masses to make the Higgs boson mass 125 GeV.

3 Neutralino-Nucleon Scattering Cross Section

Here we give formulae for the calculation of the scattering cross section of the neutralino with nucleon [25, 28, 29]. It is calculated from the effective Lagrangian for scattering of the neutralino with quarks and gluon in the limit of low relative velocity, which is given by

$$\begin{aligned}
\mathcal{L}_{\rm eff} &= d_q\,\overline{\tilde{\chi}^0}\gamma^\mu\gamma_5\tilde{\chi}^0\;\bar{q}\gamma_\mu\gamma_5 q + f_q m_q\,\overline{\tilde{\chi}^0}\tilde{\chi}^0\;\bar{q}q \\
&+ \frac{g_q^{(1)}}{M}\,\overline{\tilde{\chi}^0}i\partial^\mu\gamma^\nu\tilde{\chi}^0\;\mathcal{O}_{\mu\nu}^q + \frac{g_q^{(2)}}{M^2}\,\overline{\tilde{\chi}^0}(i\partial^\mu)(i\partial^\nu)\tilde{\chi}^0\;\mathcal{O}_{\mu\nu}^q \\
&+ f_G\,\overline{\tilde{\chi}^0}\tilde{\chi}^0 G_{\mu\nu}^a G^{a\mu\nu} + \frac{g_G^{(1)}}{M}\,\overline{\tilde{\chi}^0}i\partial^\mu\gamma^\nu\tilde{\chi}^0\;\mathcal{O}_{\mu\nu}^g + \frac{g_G^{(2)}}{M^2}\,\overline{\tilde{\chi}^0}(i\partial^\mu)(i\partial^\nu)\tilde{\chi}^0\;\mathcal{O}_{\mu\nu}^g\,,
\end{aligned} \tag{3}$$

where M and m_q are the masses of the neutralino and quarks, respectively. Sum over quark flavors $q = u, d, s$ for the first and second terms and $q = u, d, s, c, b$ for the third

[2] Threshold correction may change the ratio M_1/M_2 from the above relation. However, this does not affect our numerical result significantly.

and fourth terms is implicit. The field strength tensor of the gluon field is denoted by $G^a_{\mu\nu}$. The last two lines include the quark and gluon twist-2 operators, $\mathcal{O}^q_{\mu\nu}$ and $\mathcal{O}^g_{\mu\nu}$, respectively, which are defined as,

$$\begin{aligned}\mathcal{O}^q_{\mu\nu} &\equiv \frac{1}{2}\bar{q}i\left[D_\mu\gamma_\nu + D_\nu\gamma_\mu - (g_{\mu\nu}/2)\not{D}\right]q \ , \\ \mathcal{O}^g_{\mu\nu} &\equiv G^{a\rho}_\mu G^a_{\rho\nu} + (g_{\mu\nu}/4)G^a_{\alpha\beta}G^{a\alpha\beta} \ , \end{aligned} \tag{4}$$

with $D_\mu \equiv \partial_\mu - ig_3 A^a_\mu T_a$ the covariant derivative (T_a is the generator of $\mathrm{SU}(3)_C$, and A^a_μ is the gluon field). In order to remove the redundant terms, we use the integration by parts and the equation of motion for the operators. The first term in Eq. (3) yields the SD interaction, while the other terms generate the SI interactions.

In order to compute the $\tilde{\chi}^0$-nucleon cross section from the effective Lagrangian, we need to evaluate the nucleon matrix elements of the quark and gluon operators. The nucleon matrix elements of the scalar-type light-quark operators, *i.e.*, $m_q\bar{q}q$ ($q = u, d, s$), are parametrized as

$$\langle N|m_q\bar{q}q|N\rangle \equiv m_N f^{(N)}_{Tq} \ , \tag{5}$$

where m_N is the nucleon mass and $|N\rangle$ denotes the one-particle state of the nucleon ($N = p, n$). For the heavy quarks and gluon, on the other hand, their matrix elements are obtained by using the trace anomaly of the energy-momentum tensor in QCD:

$$\begin{aligned}\langle N|m_Q\bar{Q}Q|N\rangle &= -\frac{\alpha_s}{12\pi}c_Q\langle N|G^a_{\mu\nu}G^{a\mu\nu}|N\rangle \ , \\ m_N f^{(N)}_{TG} &= -\frac{9\alpha_s}{8\pi}\langle N|G^a_{\mu\nu}G^{a\mu\nu}|N\rangle \ , \end{aligned} \tag{6}$$

with $f^{(N)}_{TG} \equiv 1 - \sum_q f^{(N)}_{Tq}$ and $\alpha_s \equiv g_3^2/4\pi$. The long-distance QCD correction c_Q in the above expression is evaluated in Ref. [30] as $c_Q = 1 + 11\alpha_s(m_Q)/4\pi$, and we take their numerical values as $c_c = 1.32$, $c_b = 1.19$ and $c_t = 1$ in this paper. As can be seen from Eq. (6), the scalar-type heavy quark operators contribute to the nucleon matrix elements only through the loop-induced gluon operator.

The nucleon matrix elements of the twist-2 operators are evaluated with the parton distribution functions (PDFs):

$$\langle N(k)|\mathcal{O}^q_{\mu\nu}|N(k)\rangle = \frac{1}{m_N}(k_\mu k_\nu - m_N^2 g_{\mu\nu}/4)\ (q_N(2) + \bar{q}_N(2)) \ , \tag{7}$$

$$\langle N(k)|\mathcal{O}^g_{\mu\nu}|N(k)\rangle = \frac{1}{m_N}(k_\mu k_\nu - m_N^2 g_{\mu\nu}/4)\ G_N(2) \ , \tag{8}$$

where $q_N(2)$, $\bar{q}_N(2)$ and $G_N(2)$ are the second moments of PDFs of quark, anti-quark and gluon, respectively, which are given by

$$\begin{aligned} q_N(2) + \bar{q}_N(2) &= \int_0^1 dx\ x\ [q_N(x) + \bar{q}_N(x)] \ , \\ G_N(2) &= \int_0^1 dx\ x\ g_N(x) \ . \end{aligned} \tag{9}$$

Here, we use the PDFs at the scale of $\mu = m_Z$ (m_Z is the Z boson mass), since, as will be described later, the terms with quark twist-2 operators in Eq. (3) are induced by the one-loop diagrams in which the loop momentum around the weak boson mass scale yields dominant contribution.

Finally, the SI effective coupling is obtained as

$$\frac{f_N}{m_N} = f_{Tq}^{(N)} f_q + \frac{3}{4}\left(q_N(2) + \bar{q}_N(2)\right)\left(g_q^{(1)} + g_q^{(2)}\right) - \frac{8\pi}{9\alpha_s} f_{TG}^{(N)} f_G + \frac{3}{4} G_N(2)\left(g_G^{(1)} + g_G^{(2)}\right). \quad (10)$$

Here the sum of quark flavors is implicit as in Eq. (3). Note the factor $1/\alpha_s$ in front of f_G in Eq. (10). It makes the gluon contribution sizable, although the interactions of the neutralino with gluon are induced by higher-loop processes than those with light quarks [25]. On the other hand, the contributions of the twist-2 operators of gluon are sub-dominant[3] as $g_G^{(1)}$ and $g_G^{(2)}$ are suppressed by the strong coupling constant α_s. Thus, we ignore them in this paper.

The effective axial vector coupling, which is relevant for the SD cross section, is readily written as

$$a_N = d_q \Delta q_N \ , \quad (11)$$

with

$$\langle N|\bar{q}\gamma_\mu\gamma_5 q|N\rangle = 2 s_\mu \Delta q_N \ . \quad (12)$$

Here s_μ is the spin of the nucleon and quark flavor sum is taken for $q = u, d, s$. By using the effective couplings obtained above, we obtain the cross section of the neutralino with nucleon:

$$\sigma_N = \frac{4}{\pi} m_R^2 \left[|f_N|^2 + 3\,|a_N|^2\right] \ , \quad (13)$$

where $m_R \equiv M m_N/(M + m_N)$ is the reduced mass of neutralino-nucleon system.

Before concluding this section, we refer to the numerical values for the parameters that we use in this paper. The mass fractions of light quarks, $f_{Tq}^{(N)}$ defined in Eq. (5), are to be extracted from the results of the lattice QCD simulations [32, 33]. The mass fractions of light quarks are evaluated with independent methods and also by independent groups so that the results derived with the lattice QCD simulations have become more reliable. The mass fractions evaluated in the chiral perturbation theory (ChPT) have larger uncertainties than those from the lattice QCD. The SI cross section evaluated by the use of the mass fractions from the ChPT, which predicts larger $f_{Ts}^{(N)}$, is shown in

[3]Evaluating the nucleon matrix elements of twist-2 operators at $\mu = m_Z$ makes the perturbative expansion with respect to α_s reliable. Instead, if one would like to estimate the matrix elements at $\mu = 1$ GeV, one also needs to take into account the operator-mixing effects due to the QCD radiative corrections, and therefore, to include the gluon twist-2 operator, as in Ref. [31]. These two approaches are equivalent since the sum of the terms with twist-2 operators is scale-independent once they are multiplied by their coefficients. Generally speaking, however, the former approach makes the calculation robust thanks to the perturbativity of the QCD coupling.

Mass fraction	
(proton)	
$f_{Tu}^{(p)}$	0.019(5)
$f_{Td}^{(p)}$	0.027(6)
$f_{Ts}^{(p)}$	0.009(22)
(neutron)	
$f_{Tu}^{(n)}$	0.013(3)
$f_{Td}^{(n)}$	0.040(9)
$f_{Ts}^{(n)}$	0.009(22)

Second moment at $\mu = m_Z$			
$u(2)$	0.22	$\bar{u}(2)$	0.034
$d(2)$	0.11	$\bar{d}(2)$	0.036
$s(2)$	0.026	$\bar{s}(2)$	0.026
$c(2)$	0.019	$\bar{c}(2)$	0.019
$b(2)$	0.012	$\bar{b}(2)$	0.012

Spin fraction	
Δu_p	0.77
Δd_p	-0.49
Δs_p	-0.15

Table 1: Parameters for quark and gluon matrix elements. Errors are shown only for the mass fractions, which are used for comparison with the cross section evaluated with the mass fraction from the ChPT.

Appendix A for comparison. The second moments of the PDFs of quarks and anti-quarks are calculated using the CTEQ parton distribution [34]. The spin fractions, Δq_N, in Eq. (12) are obtained from Ref. [35]. In Table 1 we list the numerical values for the mass fractions of both proton and neutron as well as the second moments of the PDFs and the spin fractions for proton. The second moments and the spin fractions for neutron are to be obtained by exchanging the values of up quark for those of down quark.

4 Results

In this section we calculate the SI cross section for the Wino-like or Higgsino-like neutralino in the high-scale SUSY scenario. The values of the Higgsino and Wino mass parameters are model-dependent. Therefore, we regard both M_2 and μ as free parameters in the following analysis while we take M_2 positive.[4]

The tree-level $\tilde{\chi}^0$-$\tilde{\chi}^0$-Higgs interaction yields scalar-type effective operators, $\overline{\tilde{\chi}^0}\tilde{\chi}^0\bar{q}q$ and $\overline{\tilde{\chi}^0}\tilde{\chi}^0 G^a_{\mu\nu}G^{a\mu\nu}$ (Left in Fig. 1). Let us denote these contributions by f_q^H and f_G^H, respectively. By adding them to the loop-level contributions[5] $f_q^{\rm EWIMP}$ and $f_G^{\rm EWIMP}$ which

[4]We assume the parameters to be real in this article. Possible phases of the parameters might affect the "Higgs" contribution, which is defined later, to the SI effective coupling.

[5]Those contributions are evaluated in a pure Wino or Higgsino limit. When $M_2 \simeq \mu$, one needs to take the mixing among them into account and modify the formulae in Ref. [26] appropriately. In the present situation, however, the tree-level contributions dominate the loop-loop level ones. Thus, the modification in the loop-level effects has no significance on the resultant scattering cross section. There exists a case where the tree-level contribution is still subdominant even when $M_2 \simeq \mu$. As we will see later, however, the lightest neutralino is almost pure gauge eigenstate in such a case. Thus the results in Ref. [26] are applicable.

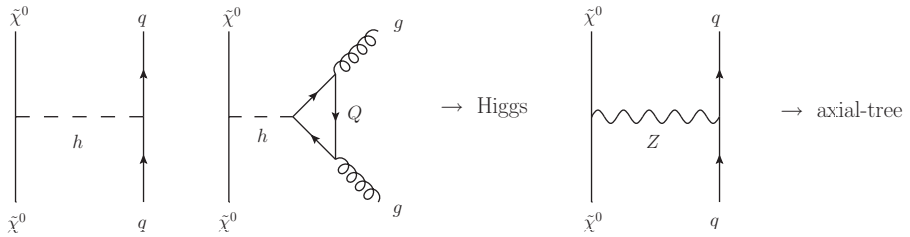

Figure 1: Diagrams via tree-level $\tilde{\chi}^0$-$\tilde{\chi}^0$-Higgs/Z interaction in elastic $\tilde{\chi}^0$-nucleon scattering. "Higgs" contribution and "axial-tree" contribution are defined in Eqs. (21) and (24).

are induced via the W/Z boson loop diagrams [26], we obtain

$$f_q = f_q^H + f_q^{\rm EWIMP}, \tag{14}$$
$$f_G = f_G^H + f_G^{\rm EWIMP}, \tag{15}$$

with

$$f_q^H = \frac{g_2^2 s^h}{4 m_W m_h^2}, \tag{16}$$
$$f_G^H = -\frac{\alpha_s}{12\pi} \sum_{Q=c,b,t} c_Q f_Q^H, \tag{17}$$

where m_W and m_h are the masses for W boson and Higgs boson, respectively. The coupling of the neutralino with the Higgs boson is denoted by s^h in the above expression, which is given as

$$s^h = (Z_{12} - Z_{11}\tan\theta_W)(Z_{13}\cos\beta - Z_{14}\sin\beta). \tag{18}$$

Here θ_W is the weak mixing angle and we take the decoupling limit since the heavier Higgs bosons have masses much larger than the weak scale. In addition, when M_2, $|\mu| \gtrsim m_W$, the coupling s^h is approximated as

$$s^h \simeq \frac{m_W}{M_2^2 - \mu^2}(M_2 + \mu \sin 2\beta), \tag{19}$$

in the Wino-like neutralino case and

$$s^h \simeq -\frac{1}{2}\left[\frac{m_W}{M_2 - |\mu|} + \frac{m_W \tan^2\theta_W}{M_1 - |\mu|}\right](1 \pm \sin 2\beta), \tag{20}$$

in the Higgsino-like neutralino case. Here the plus (minus) sign in front of $\sin 2\beta$ is for $\mu > 0$ ($\mu < 0$).[6]

[6]There is an sign error in Eq. (24) of Ref. [36] for $\mu < 0$ case. In addition, for heavy Higgs coupling, the correct expression is $\pm\frac{1}{2}\left[\frac{m_W}{M_2-|\mu|} + \frac{m_W \tan^2\theta_W}{M_1-|\mu|}\right]\cos 2\beta$.

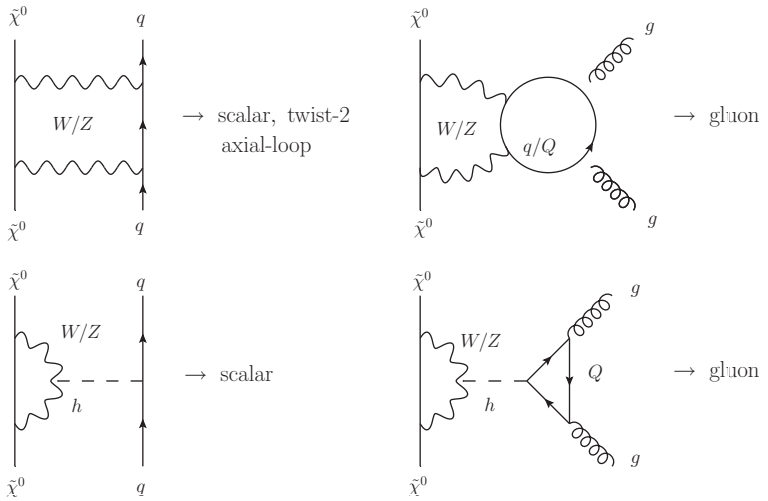

Figure 2: Diagrams which are induced by electroweak interaction in elastic $\tilde{\chi}^0$-nucleon scattering. "scalar", "twist-2", "gluon" and "axial-loop" correspond to each term in the effective couplings. Their definitions are given in Eqs. (21) and (24). A complete set of diagrams is given in Ref. [26].

As it is seen in Eqs. (19) and (20), in the case where one mass parameter is much larger than the other (*i.e.*, $M_2 \ll |\mu|$ or $|\mu| \ll M_2$), the lightest neutralino becomes almost pure Wino or Higgsino state. Then the tree-level $\tilde{\chi}^0$-$\tilde{\chi}^0$-Higgs interaction, as well as $\tilde{\chi}^0$-$\tilde{\chi}^0$-Z interaction which is relevant for the SD scattering, is suppressed. Thus the loop-level processes become important. The loop-level effective couplings are calculated in the previous work [26], where the elastic scattering cross section for generic electroweak-interacting DM particles (*i.e.*, n-tuplet of $\mathrm{SU}(2)_L$ with hypercharge Y of $\mathrm{U}(1)_Y$) is evaluated. Pure Wino corresponds to $n = 3$ and $Y = 0$, while pure Higgsino corresponds to $n = 2$ with $Y = 1/2$. The previous results have revealed that the loop-level contributions are sizable when the DM-particle mass is much larger than those of weak bosons. (See also Ref. [36].) Further, it has been found that the SI cross section tends to be suppressed with the 125 GeV Higgs boson mass due to an accidental cancellation. (See Fig. 5 of Ref. [26].) These observations indicate that both the tree-level and the loop-level contributions are significant in a wide range of parameter space. Taking the above discussion into account, we calculate the scattering cross section of the neutralino with nucleon including all the possibly dominant contributions.

For later discussion, we refer to each term in Eq. (3) as,

$$\begin{aligned}\frac{f_N}{m_N} &= f_{Tq}^{(N)} f_q^{\mathrm{EWIMP}} + \frac{3}{4}\left(q_N(2) + \bar{q}_N(2)\right)\left(g_q^{(1)} + g_q^{(2)}\right) - \frac{8\pi}{9\alpha_s} f_{TG}^{(N)} f_G^{\mathrm{EWIMP}} \\ &\quad + \left(f_{Tq}^{(N)} f_q^H - \frac{8\pi}{9\alpha_s} f_{TG}^{(N)} f_G^H\right) \\ &\equiv [(\text{scalar}) + (\text{twist-2}) + (\text{gluon}) + (\text{Higgs})]\,/m_N. \end{aligned} \tag{21}$$

Here "scalar", "twist-2" and "gluon" contributions are from diagrams in Fig. 2, while we define "Higgs" contribution, which contains both f_q^H and f_G^H, as shown in Fig. 1.

Before turning to numerical calculations, we briefly discuss the gaugino-sfermion-fermion couplings, which we call the gaugino couplings hereafter, in the high-scale SUSY scenario. The gaugino couplings are equal to the gauge couplings at the energy scale larger than $M_{\rm SUSY}$. With the scalar particles decoupled at $M_{\rm SUSY}$, however, the effective theory below the scale is not supersymmetric anymore; thus the gaugino couplings might in general deviate from the relations. This deviation affects the neutralino mass matrix, leading to corrections to Z_{ij}. Using the renormalization group equations for the gaugino couplings in the split SUSY scenario given in Ref. [7], we explicitly calculate the running of the couplings and find that the deviation of gaugino couplings from the corresponding gauge couplings is less than a few %; *e.g.*, the $\mathrm{U}(1)_Y$ gaugino coupling decreases from the supersymmetric one by around 7%, while the $\mathrm{SU}(2)_L$ gaugino coupling increases by about 1%, when $M_{\rm SUSY}$ is 10^3 TeV and $\tan\beta = 1$, which gives the Higgs mass of around 125 GeV.

Now we are ready to give numerical results of the scattering cross section. Fig. 3 shows the results of the SI scattering for the Wino-like neutralino. Here we give the cross section of the neutralino with proton. In the plots we take $M_2 = 3$ TeV and $m_h = 125$ GeV and $\mu < 0$ ($\mu > 0$) for the top (bottom) panel. $\tan\beta = 1.1$, 2 and 50 are taken in left, middle and right panels, respectively.[7] In the plot of the SI cross section, green dashed lines indicate the SI cross section with only the Higgs contribution taken into consideration, while purple solid lines show the result with all the leading contributions included. Shaded regions imply error coming from the mass fractions. It is found that the loop contribution is important in wide range of parameter space. Let us see $\mu < 0$ case first. When $\tan\beta \lesssim 2$, the Higgs contribution scales as $\propto s^h \simeq m_W/(M_2 + |\mu|)$ from Eq. (19), which does not grow as $|\mu| - M_2$ gets smaller. As a consequence, the loop contribution is comparable or larger than the Higgs contribution, depending on $|\mu| - M_2$. This behavior is seen in the plot of f_p in Fig. 4. Here we give the plot of each contribution defined in Eq. (21). In the plot result for $\tan\beta = 50$ is given for scalar, twist-2 and gluon contributions (though they are insensitive to $\tan\beta$), and results for $\tan\beta = 1.1$, 2, 5 and 50 are given for the Higgs contribution from top to bottom. Since the Higgs contribution is always positive for $\tan\beta \simeq 1.1$, it interferes constructively to the other contributions. When $\tan\beta \gg 1$, on the other hand, situation gets changed. In this case the Higgs contribution is sensitive to M_2 and $|\mu| - M_2$ for given $\tan\beta$. This fact can be seen from Eq. (19). Now s^h is given as $s^h \simeq m_W \frac{M_2 - 2|\mu|/\tan\beta}{M_2^2 - \mu^2}$. Thus the Higgs contribution is negative when $|\mu| \lesssim M_2 \tan\beta/2$ and flips its sign in larger $|\mu|$ region. This causes an cancellation; as $|\mu| - M_2$ gets larger, the absolute value of the tree-level Higgs exchanging contribution drops, and all the negative contributions cancel the positive twist-2 contribution around $|\mu| - M_2 \sim$ a few hundred

[7] Note that when $\tan\beta = 1$ the tree-level axial coupling, as well as the tree-level Higgs coupling for the Higgsino-like DM for negative μ, vanishes exactly. However, it is not the realistic case. In fact the gaugino coupling in the neutralino mass matrix receives a correction from renormalization-group effects from high scale, which we discussed above, and as a consequence the tree-level couplings do not vanish. For the purpose of studying tree- and loop-level contributions in general, we simply avoid $\tan\beta = 1$.

GeV to a few TeV, depending on $\tan\beta$. We have checked that the result is almost the same when $\tan\beta \gtrsim 5$.

When $\mu > 0$, on the contrary, the Higgs contribution is always negative. The right panel in Fig. 4 shows it for $\tan\beta = 1.1$, 2, 5 and 50 from bottom to top. Thus resultant cross section is similar to those in the case of large $\tan\beta$ and $\mu < 0$. In both $\mu < 0$ and $\mu > 0$ cases, the Higgs contribution becomes irrelevant and the loop contribution dominates the cross section when $|\mu| - M_2 \gtrsim 10$ TeV. Then the SI cross section lies around a value of $\sim 10^{-47}$ cm^2, which is consistent with the results in Refs. [24–26].

We have checked the SI cross section is almost independent of the neutralino mass except for $\mu < 0$ and low $\tan\beta$. We also give the result for $M_2 = 200$ GeV in Figs. 5 and 6. Here we take the other parameters the same as those in Fig. 3. In this case, the Higgs contribution becomes larger, leading to a bit enhanced SI cross section. However, with relatively large $\tan\beta$, a cancellation happens then the cross section behaves similar to the previous results, as it is seen in the figure.

Next let us discuss the Higgsino-like neutralino case. The results are shown in Figs. 7 and 8. Here we take $|\mu| = 1$ TeV and $m_h = 125$ GeV. The upper and lower panels correspond to $\mu < 0$ and $\mu > 0$ cases, respectively. $\tan\beta$ is taken as similarly to that in Figs. 3 and 4. In the $\mu < 0$ case, the Higgs contribution is suppressed by $(1 - \sin 2\beta)$ for $\tan\beta \simeq 1$, then the loop contributions become dominant. This is clearly seen in Fig. 8. The cross section is around 10^{-49} cm^2 in the region $M_2 - |\mu| \gtrsim 500$ GeV. When $\tan\beta$ is larger, the Higgs contribution scales as $s^h \simeq -m_W/(M_2 - |\mu|)$ and becomes dominant in the effective coupling in the region $M_2 - |\mu| \lesssim$ a few TeV to 10 TeV, depending on $\tan\beta$. In this case a cancellation occurs around $M_2 - |\mu| \sim$ a few dozens of TeV, and the SI cross section is about 10^{-49} cm^2 for larger values of $M_2 - |\mu|$. Similar cancellation is observed for the $\mu > 0$ case. In the $\mu > 0$ case, the Higgs contribution is not suppressed around $\tan\beta \simeq 1$ in contrast to $\mu < 0$ case. That is why a significant cancellation always happens.

Here we briefly comment on contributions by the heavy Higgs boson, which we did not take into account. The heavy Higgs-$\tilde{\chi}^0$-$\tilde{\chi}^0$ coupling s^H is given by $s^H \simeq -\frac{m_W \mu}{M_2^2 - \mu^2} \cos 2\beta$ for the Wino-like neutralino and $s^H \simeq \pm\frac{1}{2}\left[\frac{m_W}{M_2 - |\mu|} + \frac{m_W \tan^2\theta_W}{M_1 - |\mu|}\right] \cos 2\beta$ for the Higgsino-like neutralino. Here the overall positive and negative signs correspond to the $\mu > 0$ and $\mu < 0$ cases, respectively. As it is seen, contributions from the heavy Higgs boson are suppressed when $\tan\beta \simeq 1$. Even when $\tan\beta \gtrsim 1$, it is suppressed by the heavy Higgs mass.

Finally, we give contour plots of the SI cross section on the $|\mu| - M_2$ plane in Fig. 9. In the plot we take $m_h = 125$ GeV. Upper and lower panels are for the cases of $\mu < 0$ and $\mu > 0$, respectively, and $\tan\beta$ is taken as 1.1, 2 and 50 from left to right in each panel. Purple solid lines are contours of the SI cross section of full calculation and green dashed lines show the ones given by the Higgs contribution only. The contours of the cross section smaller than 10^{-49} cm^2 are not shown here. In the figure, dark-shaded regions are excluded by the XENON100 experiment [37]. The blue dot-dashed lines and light shaded regions correspond to prospected reaches of future experiments. To evaluate those

sensitivity limit, we use a value of 10^{-47} cm^2 and 10^{-48} cm^2 at a DM-particle mass of 60 GeV and rescale it with respect to the DM-particle mass. The former value is based on a discovery sensitivity in a ton-year experiment,[8] while the latter comes from the fact that a sensitivity for the cross section of less than 10^{-48} cm^2 is difficult to be achieved due to atmospheric neutrino background [38].

In the Wino-like neutralino region, it is seen that the full calculation deviates from the one given by the Higgs contribution significantly. This is due to the suppression of the Higgs contribution (especially for the $\mu < 0$ and $\tan\beta \sim 1$ case) or the cancellation in the effective coupling. In addition, as we discussed previously, the cross section can be enhanced due to constructive interference between the Higgs and twist-2 contributions in the $\mu < 0$, $M_2 \lesssim$ TeV and low $\tan\beta$ region (See left and middle in upper panel). Thus such a region can be probed in the future experiment even when $|\mu|$ is as large as a dozens of TeV. If much better sensitivity was accomplished, larger $|\mu|$ could be also studied.

For the Higgsino-like case, the Higgs contribution almost determines the cross section in the region where future experiments may reach. The loop effect becomes important when the the Higgs contribution is suppressed (for $\mu < 0$ and $\tan\beta \simeq 1$ case) or in the region where M_2 is above several TeV. For the $\mu < 0$ and $\tan\beta \simeq 1$ case, the cross section is around 10^{-49} cm^2 thus it is far below the sensitivity of future experiments.

5 Conclusion

The high-scale supersymmetry, in which SUSY particles are much heavier than the weak scale except for gauginos and/or Higgsino, is favored from viewpoints of the discovered 125 GeV Higgs boson, null results in the SUSY particle searches at the LHC, and the SUSY FCNC and CP problems. In this scenario, the Wino-like or Higgsino-like neutralino is a good candidate for the dark matter in the universe. While Wino with a mass of 2.7–3.0 TeV or Higgsino with a mass of 1 TeV is predicted in the thermal relic scenario, the non-thermal production may explain the observed dark matter abundance in even lighter mass. In this scenario, the elastic scattering of the neutralino with nucleon, relevant to the direct dark matter search experiments, is induced by tree-level Higgs boson exchange diagrams and also loop diagrams due to the electroweak interaction.

In this article, we evaluate the SI cross section of the Wino-like or Higgsino-like neutralino including contribution from the loop diagrams of the weak bosons. Since the loop diagrams are not suppressed by the neutralino mass, they may be comparable to or even dominate over the Higgs-exchange contribution, especially for the Wino-like neutralino. As a result, the SI cross section is sensitive to the sign of μ and $\tan\beta$, in addition to absolute values of the Higgsino and Wino mass parameters since the diagrams are constructively or destructively interfered with each other.

Due to atmospheric neutrino background, it is difficult to discover the DM in the direct detection experiments when the SI cross section is smaller than 10^{-48} cm^2 at a DM-particle

[8] For reference, 8.6×10^{-48} cm^2 at a DM-particle mass of ~ 60 GeV is the sensitivity of 90% C.L. discovery at a ton-year Xenon target experiment [38].

mass around 60 GeV. We found that the prediction for the SI cross section is larger than the limit in broad parameter region. (See Fig. 9.) The large-scale experiments for the direct DM detection are hopeful.

Acknowledgments

We would like to thank Tomohiro Takesako for collaboration and discussion in the early stages of this work. We are also grateful to Satoshi Shirai for useful comments. This work is supported by Grant-in-Aid for Scientific research from the Ministry of Education, Science, Sports, and Culture (MEXT), Japan, No. 20244037, No. 20540252, No. 22244021 and No.23104011 (JH), and also by World Premier International Research Center Initiative (WPI Initiative), MEXT, Japan. This work was also supported in part by the U.S. Department of Energy under contract No. DE-FG02-92ER40701, and by the Gordon and Betty Moore Foundation (KI). The work of NN is supported by Research Fellowships of the Japan Society for the Promotion of Science for Young Scientists.

A Spin-independent Cross Section Evaluated with Mass Fraction from Chiral Perturbation

In this paper we have used the input parameters extracted from the lattice QCD simulations for the mass fractions $f_{Tq}^{(N)}$. As a result, the error of the calculation is small, as we have seen above. However, another result is also reported for the mass fractions based on the chiral perturbation theory. In this case the mass fractions for proton are given as $f_{Tu}^{(p)} = 0.024(4)$, $f_{Td}^{(p)} = 0.041(6)$ and $f_{Ts}^{(p)} = 0.40(14)$ [39, 40]. Large discrepancy[9] is seen for $f_{Ts}^{(p)}$, as well as larger error. To see the impact of the mass fractions on the SI cross section, we plot the results using the mass fractions extracted from the ChPT (and the other parameters are unchanged) in Figs. 10 and 11 for the Wino-like case, and Figs. 12 and 13 for the Higgsino-like case. In both cases we find that the theoretical error of the cross section is much larger than those presented in Figs. 3 and 7. Let us see the Wino-like neutralino case, for example. The SI cross section has error of an order of magnitude when $|\mu| - M_2 \gtrsim 10$ TeV (a few TeV) for $\tan\beta = 1.1$ (50), and what is worse, the lower value is undetermined for the larger values of $|\mu|$. In the Higgsino-like case, it is seen the error is much larger than those in the result which is based on the lattice QCD simulation. Therefore, we conclude that in using the input of the mass fractions based on the ChPT the SI cross section can not be predicted due to the large uncertainty.

[9]However, a recent calculation based on the covariant baryon chiral perturbation theory in Ref. [41] gives a smaller value for the strangeness content of nucleon than those in the previous works. Indeed, it is consistent with the lattice results, while its error is much larger than those with the lattice simulations.

B Spin-dependent Cross Section

For completeness, we show the results for the SD cross section. In the case of the SD scattering, the tree-level axial vector coupling is induced through the Z boson exchange. With the loop-level contribution combined, the axial vector coupling is given as

$$d_q = d_q^{\rm tree} + d_q^{\rm EWIMP}. \tag{22}$$

Here $d_q^{\rm EWIMP}$ is taken from Eq. (4.3) in Ref. [26], and the tree-level contribution is

$$d_q^{\rm tree} = \frac{g_2^2}{8m_W^2}(|Z_{13}|^2 - |Z_{14}|^2)\ T_q^3, \tag{23}$$

with T_q^3 the weak isospin of light quarks. Then as in f_N, we call each term in Eq. (11),

$$\begin{aligned} a_N &= d^{\rm tree}\Delta q_N + d^{\rm EWIMP}\Delta q_N \\ &\equiv \text{(axial-tree)} + \text{(axial-loop)}. \end{aligned} \tag{24}$$

The first term is derived from the W/Z box diagrams shown in Fig. 2, while the second term is given in the tree-level Z exchange (the right diagram in Fig. 1).

The SD cross section for the Wino-like and Higgsino-like cases are presented in Fig. 14, while the effective axial coupling is given in Fig. 15. In the plots we take the same values for the SUSY parameters as those in Fig. 3 and Fig. 7 for the Wino-like and Higgsino-like cases, respectively. As is obvious from Eq. (23), the result is independent of the sign of μ. In both cases, tree-level and loop-level couplings are constructive. While the tree-level contribution highly depends on $\tan\beta$ when $\tan\beta \lesssim 10$, it turns out to be insensitive to $\tan\beta$ otherwise. The SD cross section obtained is are so small that there is little hope to detect DM via the SD interactions in the future experiments.

References

[1] G. Aad *et al.* [ATLAS Collaboration], arXiv:1208.0949 [hep-ex];
S. Chatrchyan *et al.* [CMS Collaboration], arXiv:1207.1898 [hep-ex].

[2] G. Aad *et al.* [ATLAS Collaboration], Phys. Lett. B **716**, 1 (2012);
S. Chatrchyan *et al.* [CMS Collaboration], Phys. Lett. B **716**, 30 (2012) .

[3] Y. Okada, M. Yamaguchi and T. Yanagida, Prog. Theor. Phys. **85**, 1 (1991);
Y. Okada, M. Yamaguchi and T. Yanagida, Phys. Lett. B **262**, 54 (1991);
H. E. Haber and R. Hempfling, Phys. Rev. Lett. **66**, 1815 (1991);
J. R. Ellis, G. Ridolfi and F. Zwirner, Phys. Lett. B **257**, 83 (1991);
J. R. Ellis, G. Ridolfi and F. Zwirner, Phys. Lett. B **262**, 477 (1991).

[4] L. J. Hall, D. Pinner and J. T. Ruderman, JHEP **1204**, 131 (2012);
A. Arbey, M. Battaglia, A. Djouadi, F. Mahmoudi and J. Quevillon, Phys. Lett. B **708**, 162 (2012);
P. Draper, P. Meade, M. Reece and D. Shih, Phys. Rev. D **85**, 095007 (2012).

[5] J. D. Wells, hep-ph/0306127.

[6] N. Arkani-Hamed and S. Dimopoulos, JHEP **0506**, 073 (2005).

[7] G. F. Giudice and A. Romanino, Nucl. Phys. B **699**, 65 (2004) [Erratum-ibid. B **706**, 65 (2005)].

[8] N. Arkani-Hamed, S. Dimopoulos, G. F. Giudice and A. Romanino, Nucl. Phys. B **709**, 3 (2005).

[9] J. D. Wells, Phys. Rev. D **71**, 015013 (2005) .

[10] L. J. Hall and Y. Nomura, JHEP **1003**, 076 (2010) .

[11] L. J. Hall and Y. Nomura, JHEP **1201**, 082 (2012) .

[12] G. F. Giudice and A. Strumia, Nucl. Phys. B **858**, 63 (2012);
M. Ibe and T. T. Yanagida, Phys. Lett. B **709**, 374 (2012);
M. Ibe, S. Matsumoto and T. T. Yanagida, Phys. Rev. D **85**, 095011 (2012).

[13] F. Gabbiani, E. Gabrielli, A. Masiero and L. Silvestrini, Nucl. Phys. B **477**, 321 (1996) .

[14] M. Fukugita and T. Yanagida, Phys. Lett. B **174**, 45 (1986);
W. Buchmuller, R. D. Peccei and T. Yanagida, Ann. Rev. Nucl. Part. Sci. **55**, 311 (2005).

[15] J. Hisano, D. Kobayashi and N. Nagata, Phys. Lett. B **716**, 406 (2012).

[16] K. S. Jeong, M. Shimosuka and M. Yamaguchi, arXiv:1112.5293 [hep-ph];
R. Saito and S. Shirai, Phys. Lett. B **713**, 237 (2012);
R. Sato, S. Shirai and K. Tobioka; arXiv:1207.3608 [hep-ph];
B. Bhattacherjee, B. Feldstein, M. Ibe, S. Matsumoto and T. T. Yanagida, arXiv:1207.5453 [hep-ph];
M. Bose and M. Dine, arXiv:1209.2488 [hep-ph];
L. J. Hall, Y. Nomura and S. Shirai, arXiv:1210.2395 [hep-ph].

[17] J. Hisano, S. Matsumoto, M. Nagai, O. Saito and M. Senami, Phys. Lett. B **646**, 34 (2007).

[18] M. Cirelli, A. Strumia and M. Tamburini, Nucl. Phys. B **787**, 152 (2007) .

[19] T. Gherghetta, G. F. Giudice and J. D. Wells, Nucl. Phys. B **559**, 27 (1999). .

[20] T. Moroi and L. Randall, Nucl. Phys. B **570**, 455 (2000) .

[21] L. Randall and R. Sundrum, Nucl. Phys. B **557**, 79 (1999);
G. F. Giudice, M. A. Luty, H. Murayama and R. Rattazzi, JHEP **9812**, 027 (1998) .

[22] B. Murakami and J. D. Wells, Phys. Rev. D **64**, 015001 (2001) .

[23] T. Moroi and K. Nakayama, Phys. Lett. B **710**, 159 (2012) .

[24] J. Hisano, K. Ishiwata and N. Nagata, Phys. Lett. B **690**, 311 (2010) .

[25] J. Hisano, K. Ishiwata and N. Nagata, Phys. Rev. D **82**, 115007 (2010).

[26] J. Hisano, K. Ishiwata, N. Nagata and T. Takesako, JHEP **1107**, 005 (2011) .

[27] R. D. Peccei and H. R. Quinn, Phys. Rev. Lett. **38**, 1440 (1977).

[28] M. Drees and M. Nojiri, Phys. Rev. D **48**, 3483 (1993).

[29] G. Jungman, M. Kamionkowski and K. Griest, Phys. Rept. **267**, 195 (1996).

[30] A. Djouadi and M. Drees, Phys. Lett. B **484**, 183 (2000).

[31] R. J. Hill and M. P. Solon, Phys. Lett. B **707**, 539 (2012) .

[32] R. D. Young and A. W. Thomas, Phys. Rev. D **81**, 014503 (2010) .

[33] H. Ohki , *et al.* [JLQCD Collaboration], arXiv:1208.4185 [hep-lat].

[34] J. Pumplin, D. R. Stump, J. Huston, H. L. Lai, P. Nadolsky and W. K. Tung, JHEP **0207**, 012 (2002) .

[35] D. Adams *et al.* [Spin Muon Collaboration], Phys. Lett. B **357**, 248 (1995).

[36] J. Hisano, S. Matsumoto, M. M. Nojiri and O. Saito, Phys. Rev. D **71**, 015007 (2005).

[37] E. Aprile *et al.* [XENON100 Collaboration], arXiv:1207.5988 [astro-ph.CO].

[38] A. Gutlein, C. Ciemniak, F. von Feilitzsch, N. Haag, M. Hofmann, C. Isaila, T. Lachenmaier and J. -C. Lanfranchi *et al.*, Astropart. Phys. **34**, 90 (2010).

[39] M. M. Pavan, I. I. Strakovsky, R. L. Workman and R. A. Arndt, PiN Newslett. **16**, 110 (2002) .

[40] B. Borasoy and U. -G. Meissner, Annals Phys. **254**, 192 (1997) .

[41] J. M. Alarcon, L. S. Geng, J. M. Camalich and J. A. Oller, arXiv:1209.2870 [hep-ph].

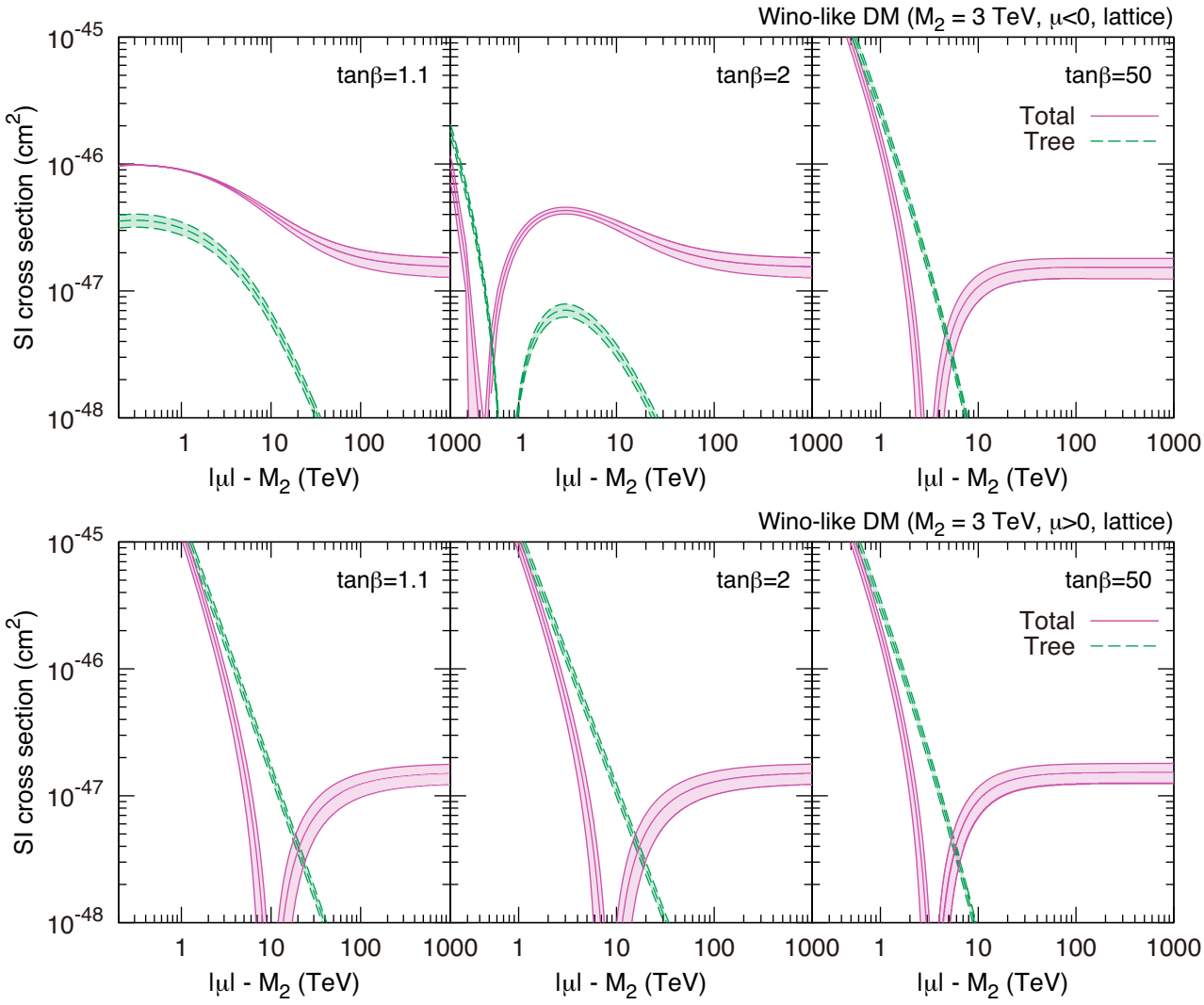

Figure 3: SI cross section of Wino-like neutralino with proton. We take $M_2 = 3$ TeV, $m_h = 125$ GeV and $\mu < 0$ (top) and $\mu > 0$ (bottom). $\tan\beta$ is taken as 1.1 (left), 2 (middle) and 50 (right) in each panel. Purple solid lines show the result from full calculation, while the result only using the Higgs contribution is in green dashed lines (color online). Shaded regions show error from the mass fractions of light quarks evaluated with the lattice QCD simulation.

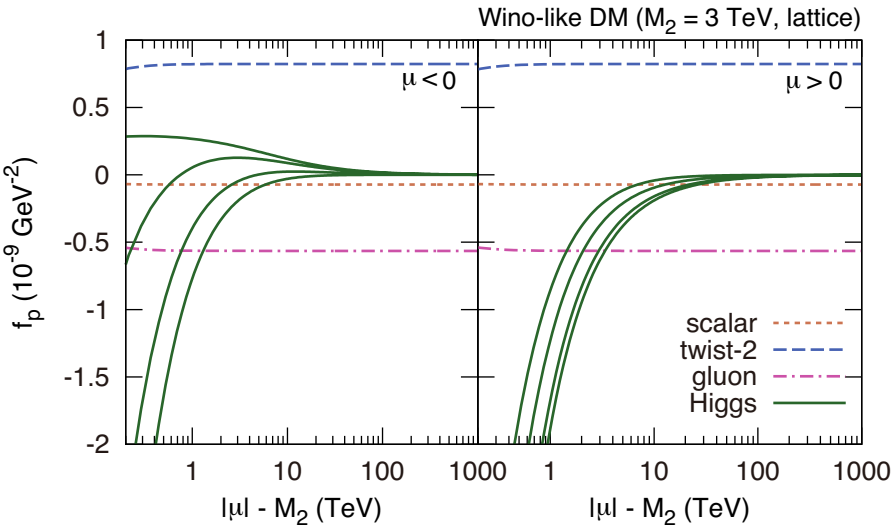

Figure 4: Each contribution in the effective coupling for Wino-like neutralino. $\mu < 0$ (left) and $\mu > 0$ (right) and the other parameters are the same as those in Fig. 3. In the panel "scalar" (orange dotted), "twist-2" (blue dashed), "gluon" (purple dot-dashed) and "Higgs" (green solid) contributions defined in Eq. (21) are given. For scalar, twist-2 and gluon contributions we take $\tan\beta = 50$, while Higgs contribution is given for $\tan\beta = 1.1$, 2, 5 and 50 from top to bottom (from bottom to top) in the left (right) panel.

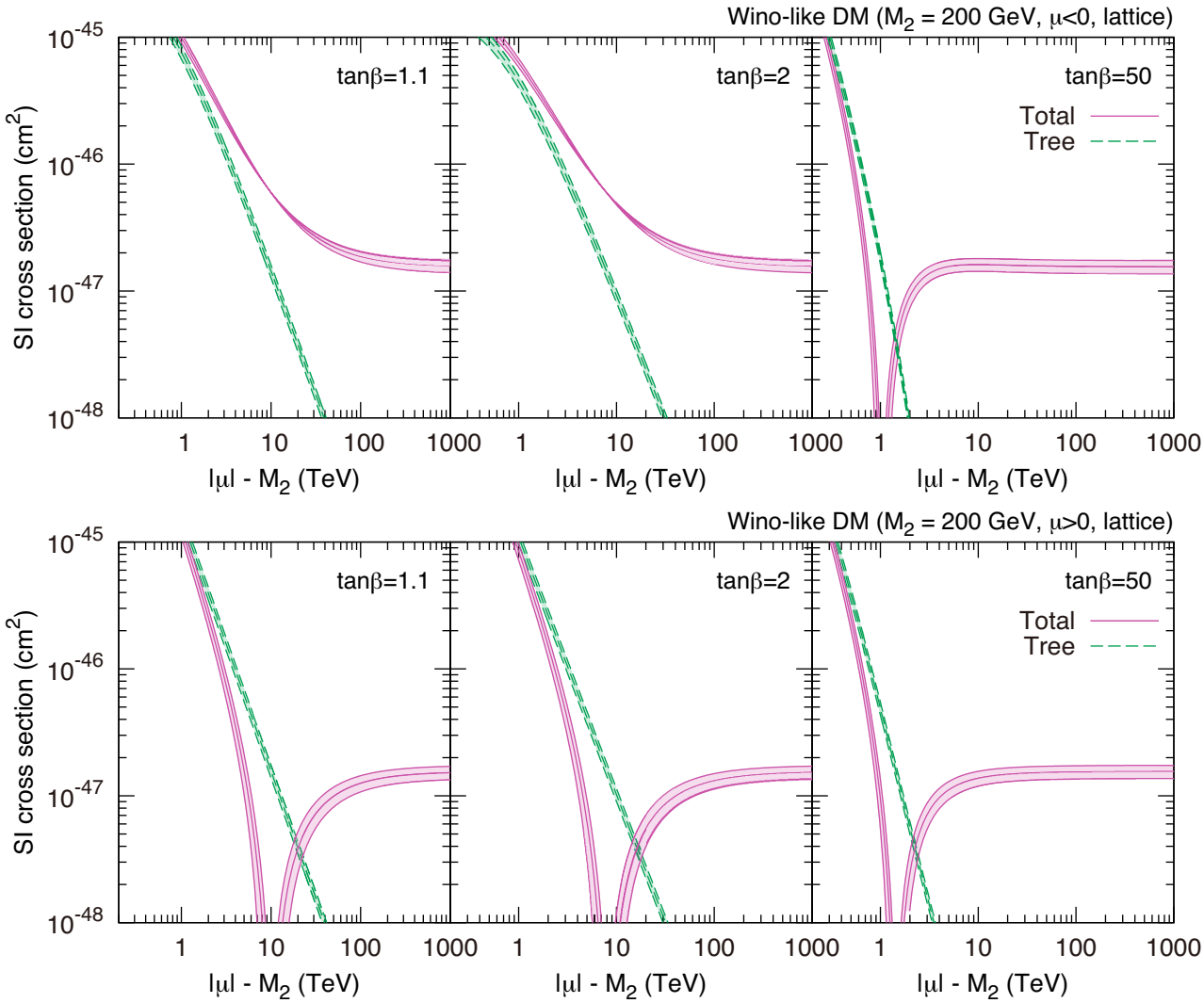

Figure 5: Similar plots to those in Fig. 3 except for taking $M_2 = 200$ GeV.

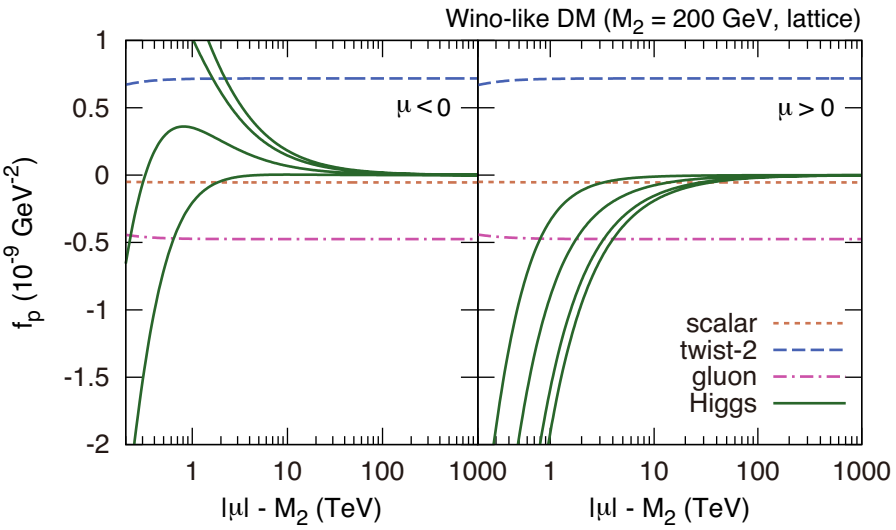

Figure 6: Similar plots to those in Fig. 4 except for taking $M_2 = 200$ GeV.

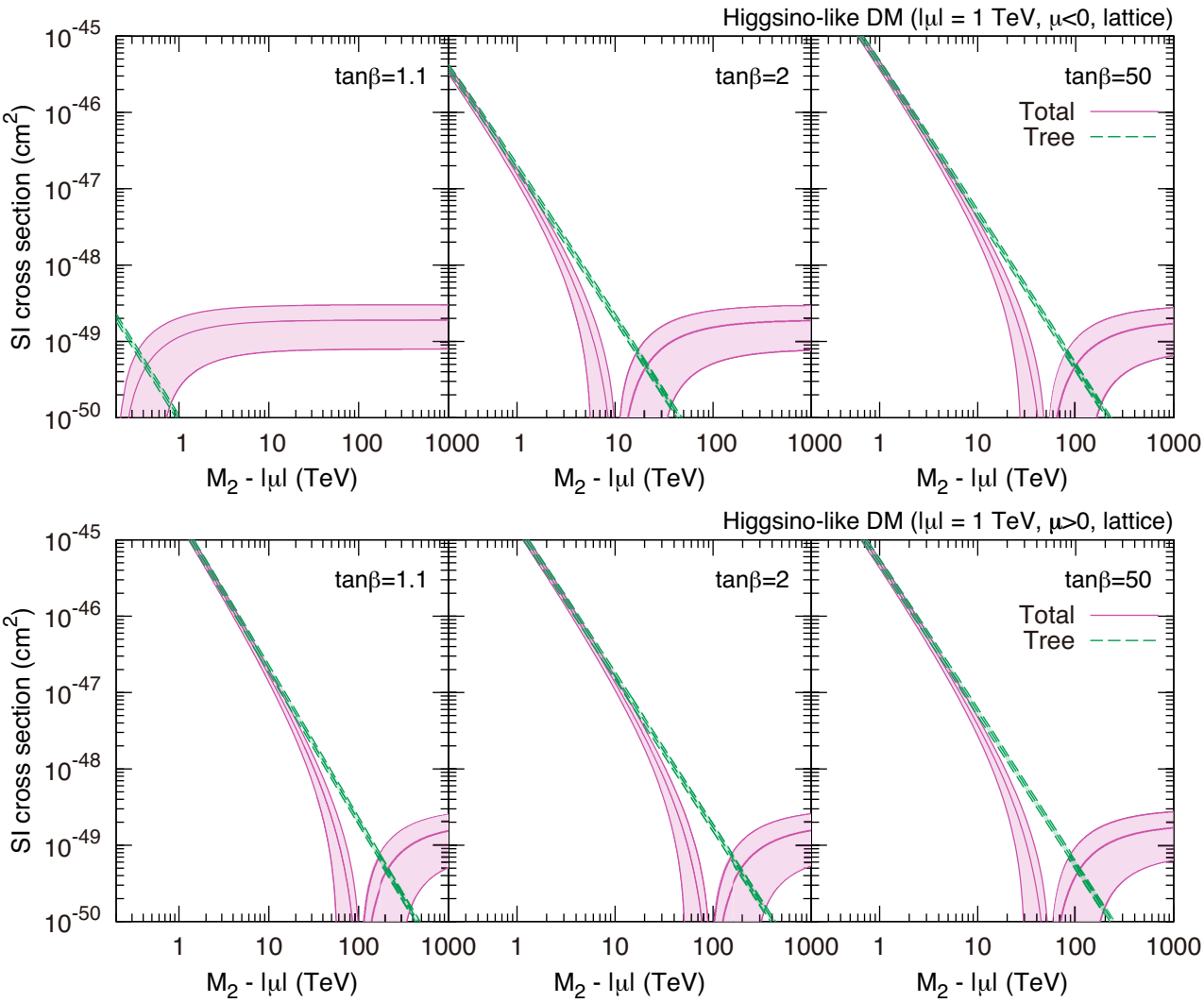

Figure 7: SI cross section of Higgsino-like neutralino with proton. We take $|\mu| = 1$ TeV, $m_h = 125$ GeV and $\mu < 0$ (top) and $\mu > 0$ (bottom). $\tan\beta$ is taken as 1.1 (left), 2 (middle) and 50 (right) in each panel. Line contents are the same as those in Fig. 3.

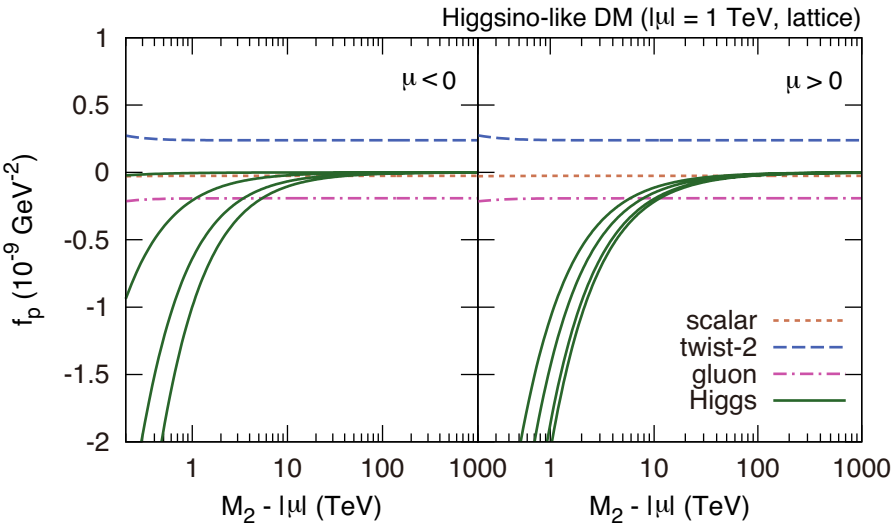

Figure 8: Each contribution in the effective coupling for Higgsino-like neutralino. $\mu < 0$ (left) and $\mu > 0$ (right) and the other parameters as well as line contents are similar to those in Fig. 7.

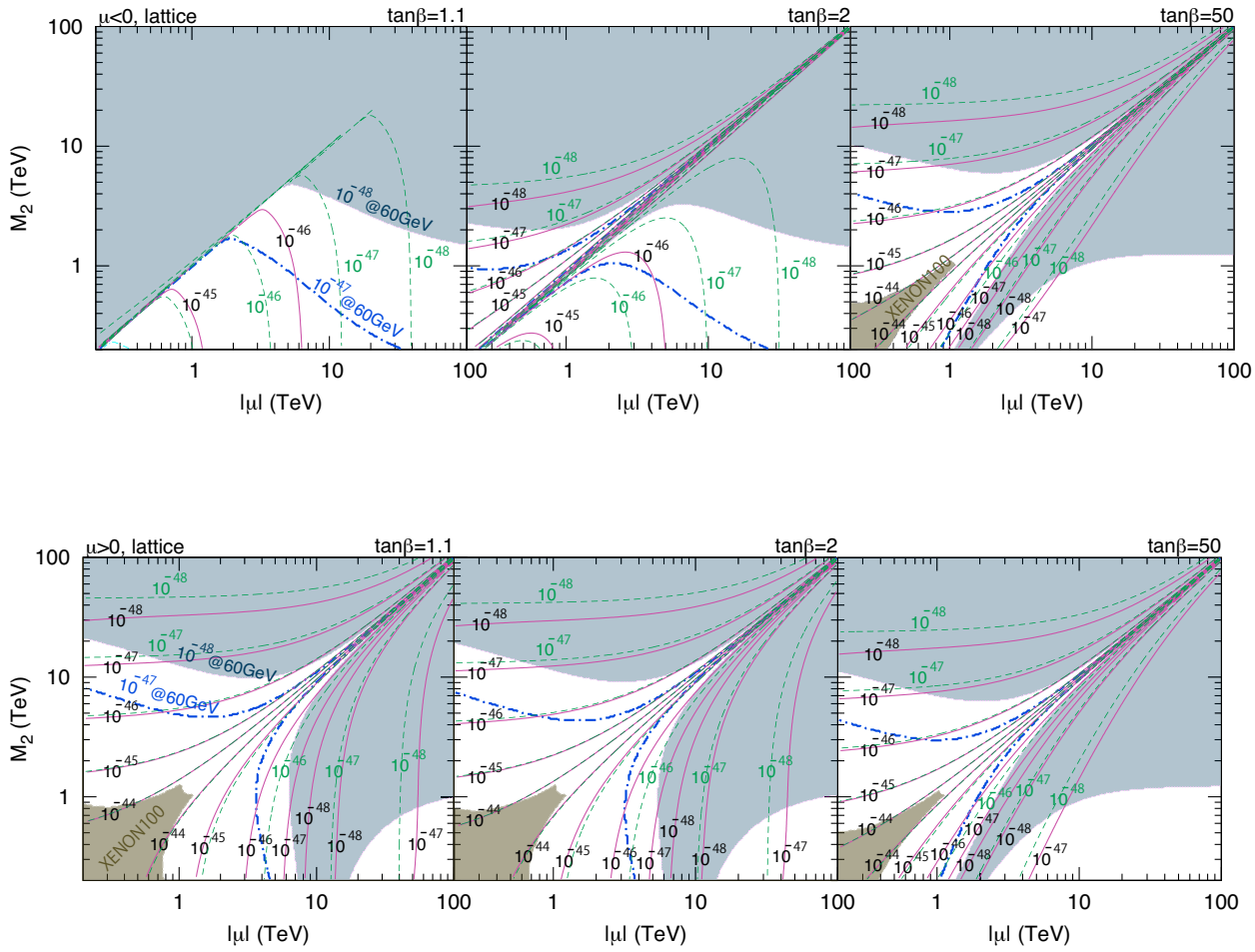

Figure 9: Contour of the SI cross section in cm^2 unit. Upper panels are in the case where $\mu < 0$ and $\tan\beta = 1.1$ (left), 2 (middle), and 10 (right) are taken, respectively. In the lower panels μ is set to be positive. We take $m_h = 125$ GeV. Results from full calculation and the only Higgs contribution are given in purple solid and green dashed lines, respectively. Lines are shown for the cross section larger than 10^{-48} cm^2. Here we also show the exclusion regions by XENON100 [37] in dark shade. Blue dot-dashed lines and light-shaded regions correspond to future prospects of experiments with sensitivities to cross section 10^{-47} cm^2 and smaller than 10^{-48} cm^2 at a DM-particle mass of ~ 60 GeV, respectively.

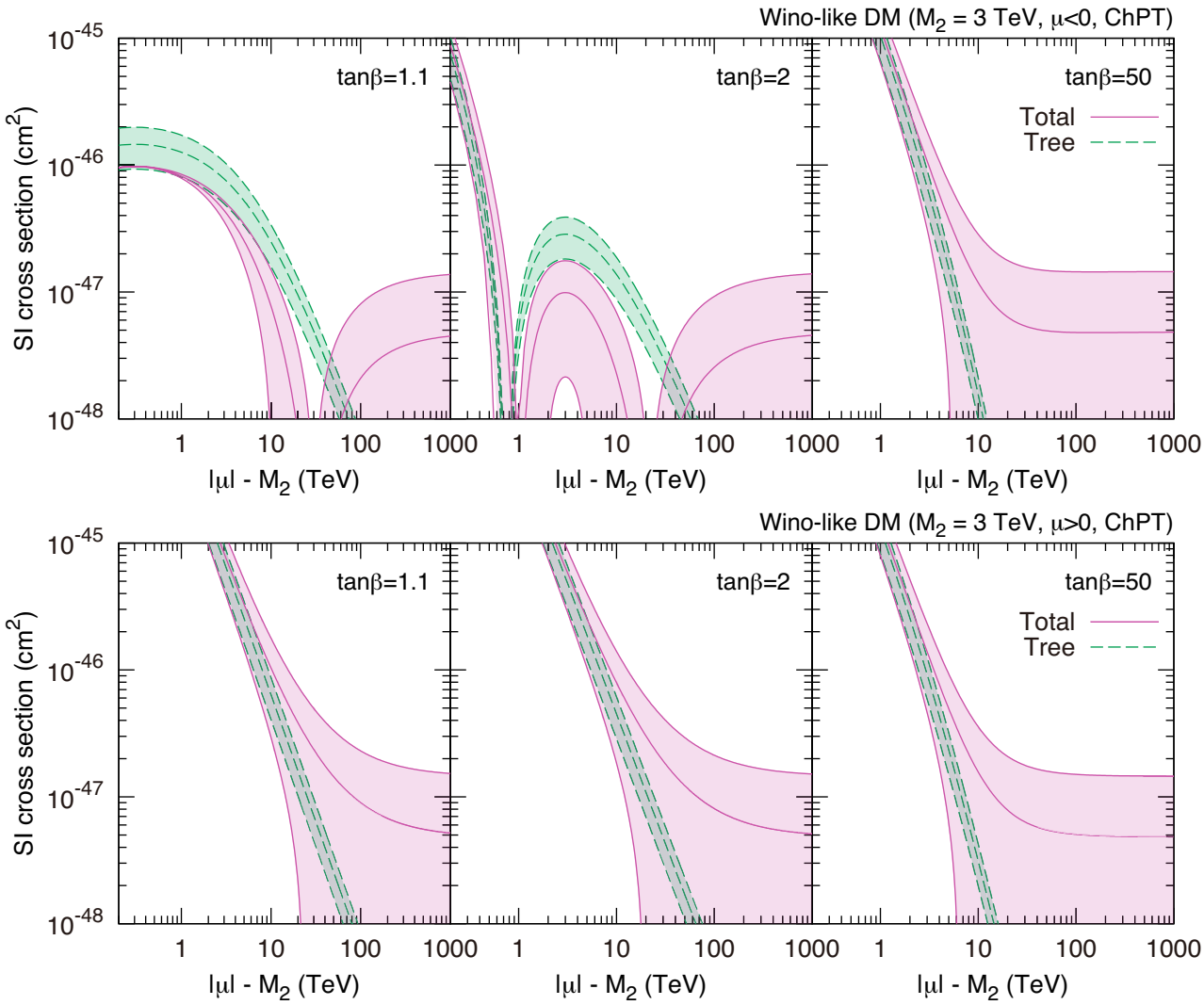

Figure 10: Similar plots to those in Fig. 3 except that the mass fractions $f_{Tq}^{(N)}$ from the ChPT are used.

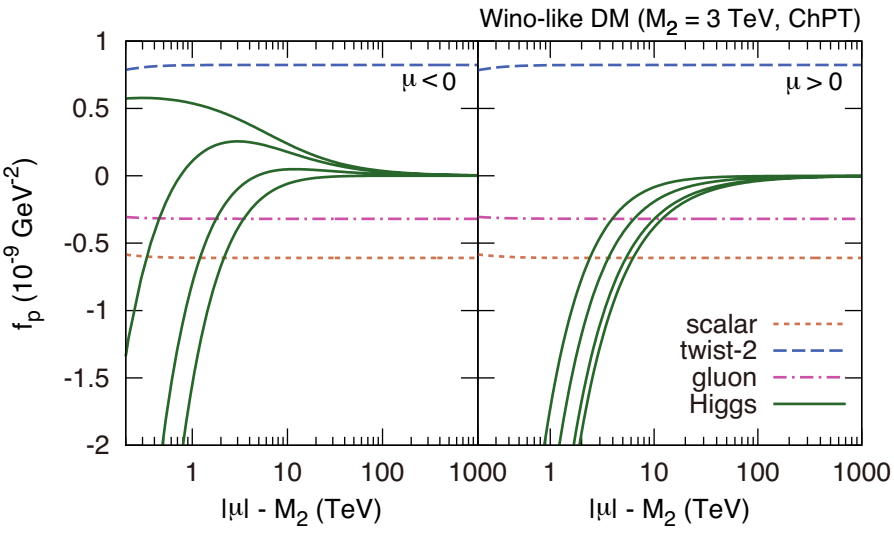

Figure 11: Similar plots to those in Fig. 4 except that the mass fractions $f_{Tq}^{(N)}$ from the ChPT are used.

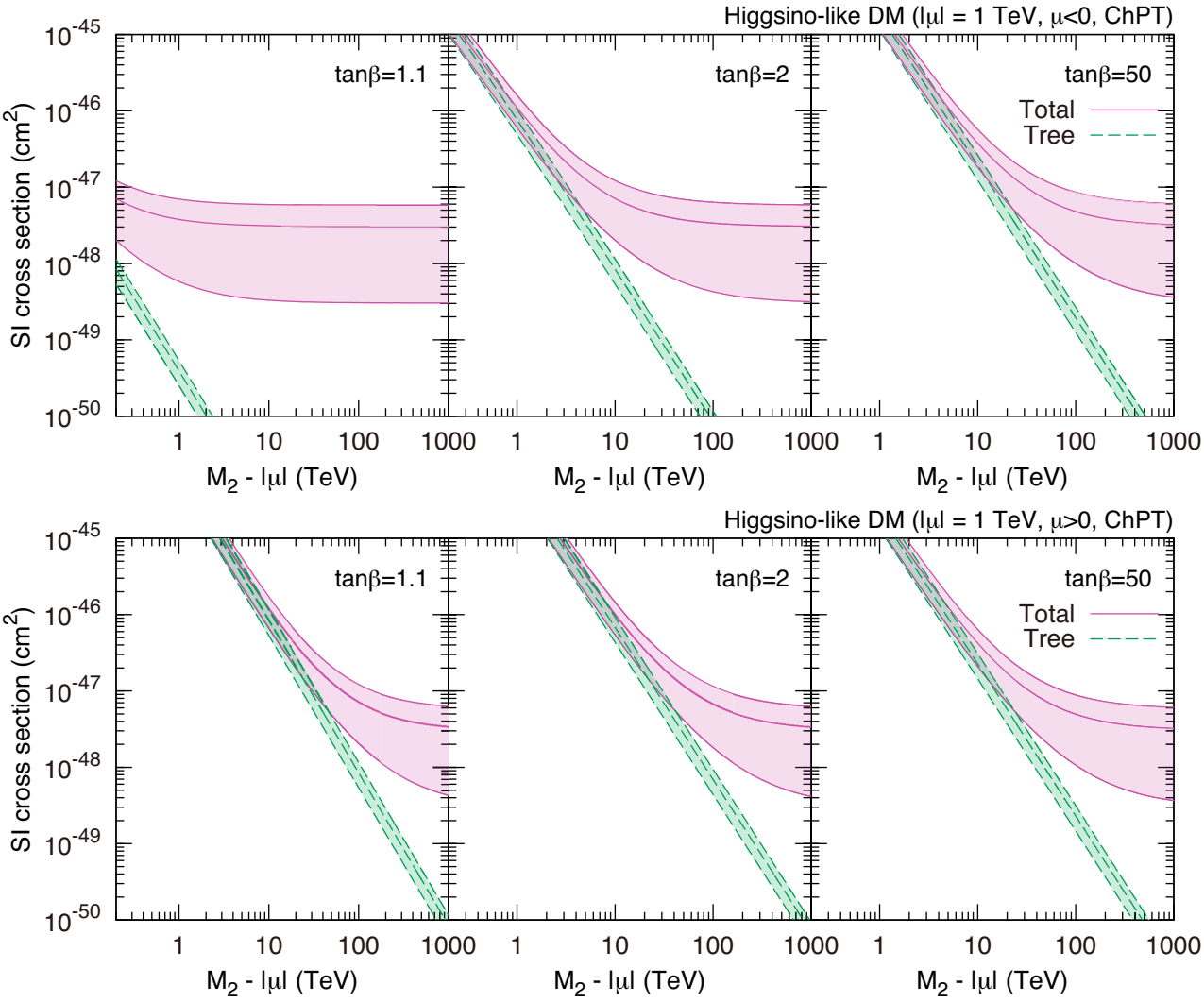

Figure 12: Similar plots to those in Fig. 7 except that the mass fractions $f_{Tq}^{(N)}$ from the ChPT are used.

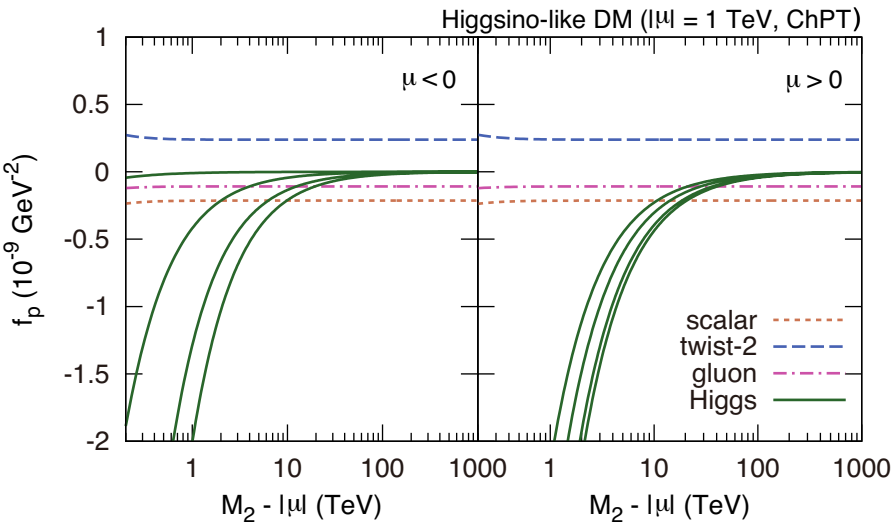

Figure 13: Similar plots to those in Fig. 8 except that the mass fractions $f_{Ts}^{(N)}$ from the ChPT are used.

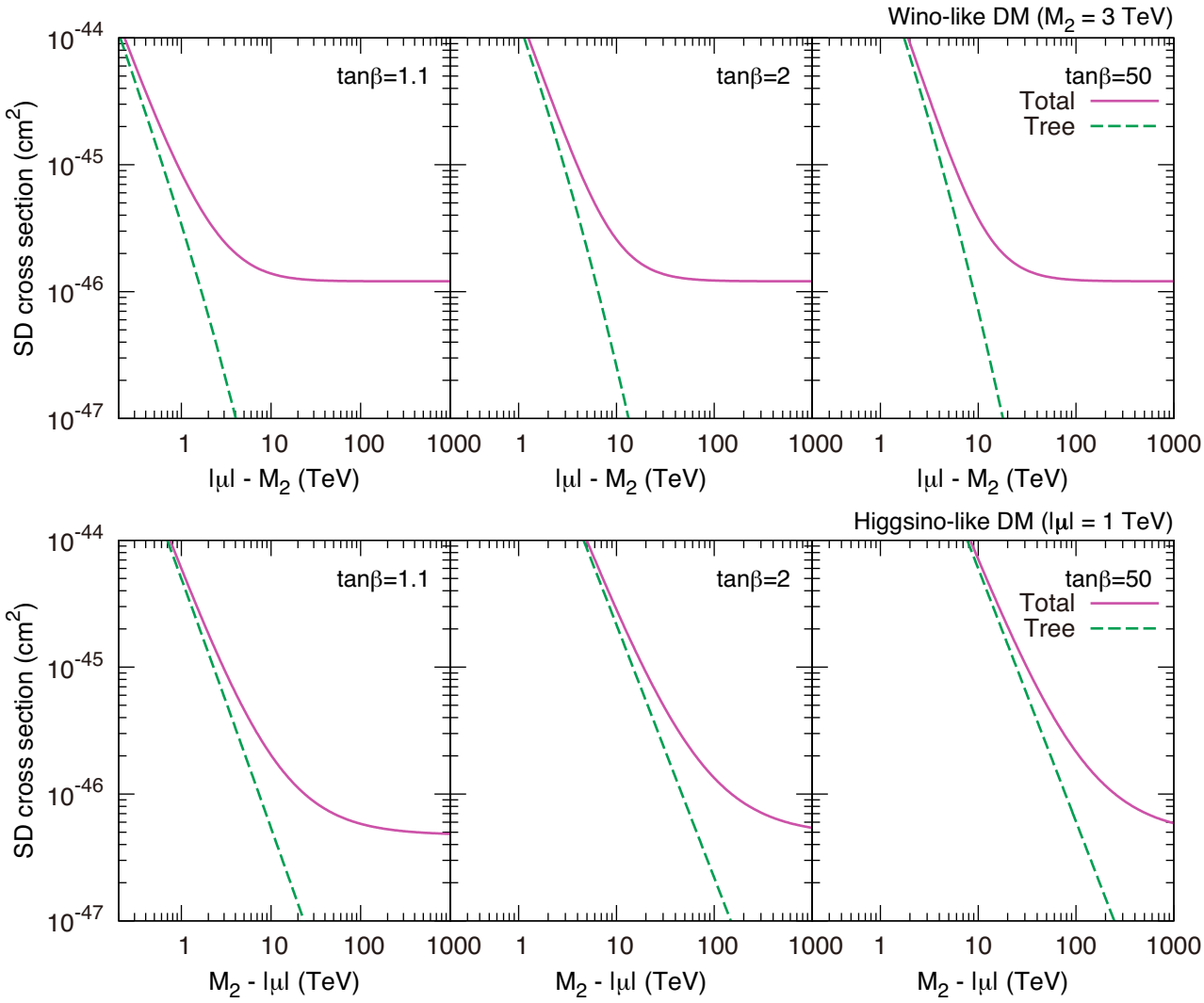

Figure 14: SD cross section for Wino-like neutralino (top) and Higgsino-like neutralino (bottom) where the input parameters are set to be the same as those in Figs. 3 and 7, respectively. Results are shown for one-loop level and tree-level in purple solid and green dashed lines, respectively.

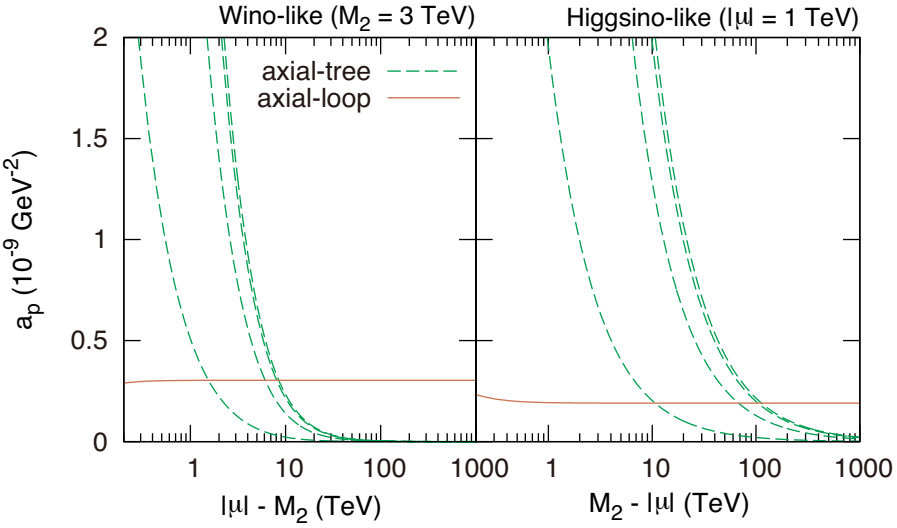

Figure 15: Each contribution in the effective axial coupling for Wino-like (left) and Higgsino-like neutralinos (right). In the figure tree-level and one-loop level contributions, defined in Eq. (24), are shown in green dashed and orange solid lines, respectively. For tree-level contribution $\tan\beta = 1.1$ 2, 5 and 50 are taken from bottom to top.